Clinical & Experimental Immunology
The Journal of Translational Immunology

Clinical and Experimental Immunology ORIGINAL ARTICLE doi:10.1111/cei.12064

Evaluation of *in vivo* T cell kinetics: use of heavy isotope labelling in type 1 diabetes

J. B. Bollyky,* S. A. Long,* M. Fitch,† P. L. Bollyky,* M. Rieck,* R. Rogers,* P. L. Samuels,* S. Sanda,* J. H. Buckner,* M. K. Hellerstein† and C. J. Greenbaum*

*Benaroya Research Institute, Seattle, WA, and †Department of Nutritional Science and Toxicology, University of California, Berkeley, CA, USA

Accepted for publication 7 January 2013
Correspondence: C. J. Greenbaum, Benaroya Research Institute, Diabetes Clinical Research Program, 1201 9th Avenue, Seattle, WA 98101, USA.
E-mail: cjgreen@benaroyaresearch.org

Summary

CD4+ memory cell development is dependent upon T cell receptor (TCR) signal strength, antigen dose and the cytokine milieu, all of which are altered in type 1 diabetes (T1D). We hypothesized that CD4+ T cell turnover would be greater in type 1 diabetes subjects compared to controls. *In vitro* studies of T cell function are unable to evaluate dynamic aspects of immune cell homoeostasis. Therefore, we used deuterium oxide (^2H_2O) to assess *in vivo* turnover of CD4+ T cell subsets in T1D ($n = 10$) and control subjects ($n = 10$). Serial samples of naive, memory and regulatory (T_{reg}) CD4+ T cell subsets were collected and enrichment of deoxyribose was determined by gas chromatography–mass spectrometry (GC–MS). Quantification of T cell turnover was performed using mathematical models to estimate fractional enrichment (f, $n = 20$), turnover rate (k, $n = 20$), proliferation (p, $n = 10$) and disappearance (d*, $n = 10$). Although turnover of T_{regs} was greater than memory and naive cells in both controls and T1D subjects, no differences were seen between T1D and controls in T_{reg} or naive kinetics. However, turnover of CD4+ memory T cells was faster in those with T1D compared to control subjects. Measurement and modelling of incorporated deuterium is useful for evaluating the *in vivo* kinetics of immune cells in T1D and could be incorporated into studies of the natural history of disease or clinical trials designed to alter the disease course. The enhanced CD4+ memory T cell turnover in T1D may be important in understanding the pathophysiology and potential treatments of autoimmune diabetes.

Keywords: deuterium oxide, heavy water, isotope labelling, memory T cell, regulatory T cell, T cell kinetics, type 1 diabetes

Introduction

CD4+ T cells are implicated in the pathogenesis of autoimmune diabetes. In murine models islet antigen-specific CD4+ T cells are required for disease and depletion of CD4+ T cells prevents disease [1]. In human type 1 diabetes (T1D), CD4+ T cells are among the cells found infiltrating the pancreatic islets [2] and human leucocyte antigen (HLA) class II alleles are associated strongly with disease risk [3]. Because of the importance of T cells in T1D pathogenesis, several studies have looked for differences in the numbers of T cells between T1D subjects and healthy controls. There is no consistent pattern of alterations in naive T cell numbers across studies [4–6]. Similarly, both increased as well as decreased numbers of memory T cells have been reported in individuals with T1D compared with controls [7]. While lack of CD4+forkhead box protein 3 (FoxP3)+ regulatory T cells (T_{reg}) results unambiguously in the early onset of autoimmune diabetes in both mouse and man [8], most studies have none the less found no difference in the number of T_{reg} present in peripheral blood of humans with and without T1D [9–11].

In contrast to these static measurements of CD4+ T cell numbers, there are indications of altered stability, proliferation and death of CD4+ T cells in autoimmune diabetes. We reported diminished maintenance of FoxP3 expression in $CD4^+CD25^+$ T_{reg} of T1D subjects [12] and we and others have found evidence of impaired signalling through

interleukin (IL)-2R, required for both T_{reg} and memory T cell homeostasis, in T1D [13–16]. Studies in mice suggest T_{reg} turnover [17,18] may have important implications for the durability of immune tolerance [19,20]. Signals that promote proliferation may break anergy in potentially autoreactive memory T cells [21], while signals that cause deletion of autoreactive T cells through activation-induced cell death may be impaired in T1D subjects, as they are in non-obese diabetic (NOD) mice [22].

There are also indications that assessments of T cell proliferation and survival *in vitro* may not correlate with *in vivo* measures [23], emphasizing the need to study T cell kinetics *in vivo*. Advances in stable isotope methodologies have created the opportunity to measure the kinetics of cell populations *in vivo* in humans. DNA labelling with heavy water (deuterium oxide, ^2H_2O) has been useful in understanding a variety of immunological processes. Others have used these techniques to study T cell kinetics in HIV [24–27], chronic lymphocytic leukaemia [28,29] and ageing [30,31]. To our knowledge, the present study is the first to evaluate T cell kinetics in subjects with autoimmune disease *in vivo*.

Methods and materials

Clinical protocol

All subjects provided written informed consent for the protocol approved by the Benaroya Research Institute Institutional Review Board. Analysis of T cell kinetics from data obtained during the initial protocol required that we assume single exponential disappearance rates of T cell subsets [26]. After 10 subjects had been studied, we modified the protocol in order to use models which do not require such an assumption, but rather allow for quantitation of proliferation and disapperance rates from measurements in samples obtained during the post-labelling period [32]. The study modifications included measurements of plasma enrichment at each blood draw, extension of the labelling period to 63 days, collection of four samples in the post-labelling period and a minor increase in the amount of heavy water (60–80 ml) consumed to assure an adequate precursor pool of deuterium.

For all participants, the stable isotope deuterium (^2H), was administered in the form of deuterium oxide, 70% (Cambridge Isotopes, Andover, MA, USA), as described previously [26,33]. Each subject was admitted to the Benaroya Research Institute Clinical Research Center (CRD) on day 0 for 24 h to receive a 480 ml priming dose of heavy water, consumed as 60 ml every 3 h. Participants were observed for dizziness, a possible effect of transient density changes in the fluid of the inner ear, and other adverse reactions; none were observed. Upon discharge from the CRC, subjects were instructed to consume 60 or 80 ml of heavy water daily for 42 or 63 days. Granulocytes and peripheral blood mononuclear cells (PBMCs) were collected at regular intervals during the labelling period in all subjects and after the labelling period in 10 subjects (Fig. 1a). Two subjects did not complete the protocol as directed, stopping heavy water consumption on days 48 and 44 instead of 63 as instructed. Table 1 lists study subjects according to clinical characteristics and study procedures.

Cell staining and separation

PBMC were isolated from 50 ml of heparinized fresh blood by Ficoll-Paque (GE Healthcare, Piscataway, NJ, USA) density gradient centrifugation. Cells were stained with either BD (Franklin Lakes, NJ, USA) anti-CD3 allophycocyanin (APC)-cyanin 7 (Cy7) and eBioscience (San Diego, CA, USA) anti-CD45RA fluorescein isothiocyanate (FITC), CD45RO phycoerythrin (PE), CD4 PE-Cy7 and CD25 APC before being sorted for naive ($CD4^+CD45RA^+CD45RO^-CD25^-$) and T memory ($CD4^+CD45RA^-CD45RO^+CD25^-$) populations, or cells were stained with BD anti-CD127 PE and eBioscience anti-CD25 FITC, CD4 PE-Cy7, and CD3 APC, then sorted for T_{reg} cells ($CD4^+CD25^+CD127^{low}$). All cells were sorted using a FACS Vantage (BD) with purity greater than 99% and analysed using Diva software (BD). Representative density plots of flow-cytometric isolation of T cell subsets are shown in Fig. 1b. Sorted cells were snap-frozen for analysis of heavy water incorporation. Available residual sorted T_{reg} samples ($n = 14$) were stained additionally for FoxP3 (Appendix Fig. A1).

Measurement of isotopic enrichment in granulocyte and T cell DNA

DNA enrichment analysis was performed as described previously [33]. Briefly, DNA was obtained from all T cell and granulocyte fractions after proteinase K digestion using DNEasy minicolumns (Qiagen Sciences, Valencia, CA, USA). Free nucleotides were prepared by enzymatic hydrolysis with S1 nuclease and acid phosphatase. Deoxyribose from purine nucleotides was derivatized for gas chromatography–mass spectrometry (GC–MS) analysis with pentafluorobenzyl hydroxylamine in acetic acid and acetic anhydride.

GC–MS analysis was performed using an Agilent model 5973/6890 GC (Agilent Technologies/Quantum Analytics, Foster City, CA, USA) in methane NCI mode, with an Agilent DB-17 column (30 m × 250 μm ID × 25 μm film thickness) under selected ion monitoring of m/z 435–437. The excess M_{+1} (EM1) mass isotopomer abundance was calculated using enriched DNA standards to correct for abundance sensitivity of mass isotopomer ratios [33]. The EM1 value represents the isotope enrichment above natural abundance due to incorporation of ^2H_2O into newly synthesized DNA (as deoxyribose).

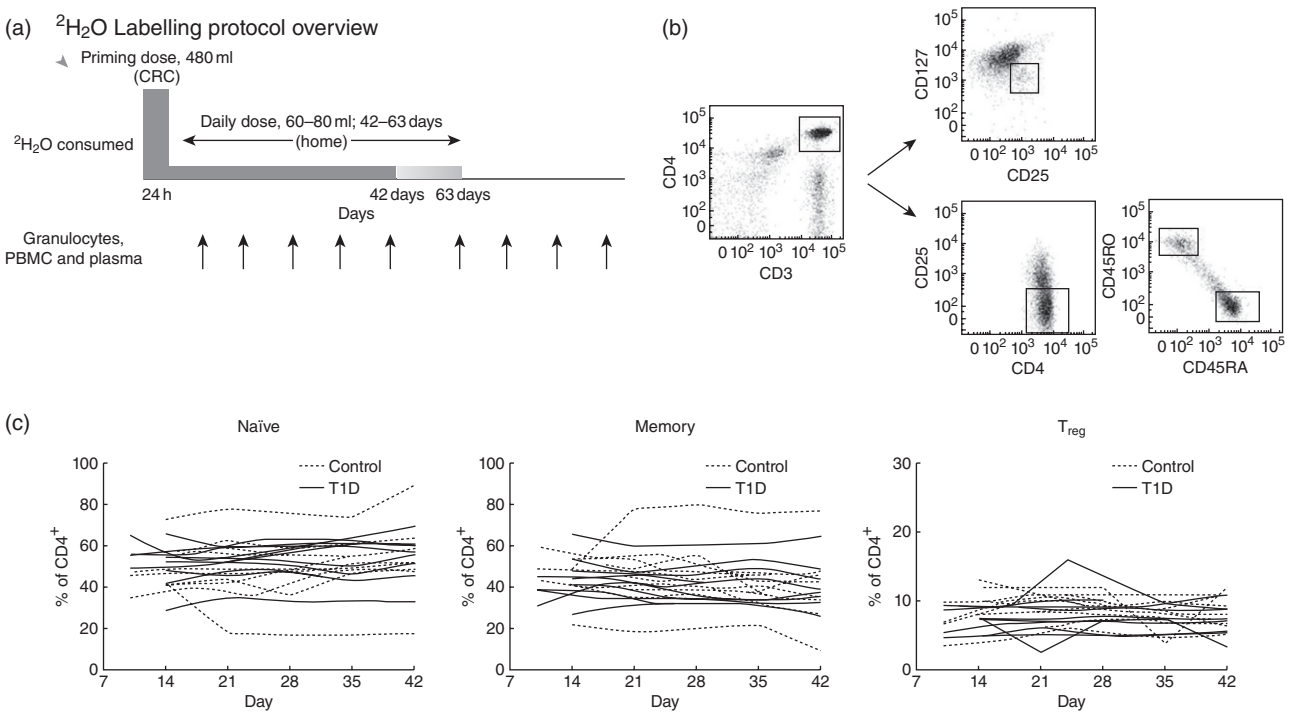

Fig. 1. (a) Deuterium-labelling protocol overview. (b) Representative density plots from flow-cytometric isolation of T cell subsets. Regulatory T cells (T_{reg}) were selected as being $CD25^+127^{low}$, $CD4^+$ memory subsets were isolated as CD25-RO+RA− and naive cells as CD25-RO-RA+. (c) T cell subset fractions over common study period (i.e. first 42 days). Solid lines represent Type 1 diabetes (T1D) subjects ($n = 10$); dashed lines represent control subjects ($n = 10$).

Measurement of plasma deuterium oxide (^2H_2O) enrichment

Plasma ^2H_2O enrichment analysis was performed as described previously [34]. Briefly, water was distilled from 100 µl aliquots of serum in inverted microvials placed in a 70°C glass bead bath. The distillate was reacted with calcium carbide chips forming acetylene gas, which was trapped and further reacted with bromine in carbon tetrachloride (0·3 M) forming tetrabromomethane. After a 2-h incubation period, excess bromine was sequestered using cyclohexene. A standard curve of % enrichment was prepared from 'stripped water' (very low ^2H_2O content) and 100% enriched ^2H_2O. GC–MS analysis was performed as above using methane PCI mode, an Agilent DB-225 column, and SIM ions of m/z 264·7–265·7.

Calculations and mathematical modelling

The kinetics of cell turnover can be characterized by determination of fractional enrichment (f), replacement rate (k), average proliferation rate (p) and disappearance rate of labelled cells (d*).

Fractional enrichment (f) and replacement rate (k)

The fractional enrichment, f, represents the fraction of newly synthesized DNA strands or, equivalently, the fraction of newly divided cells [33]. The mean f of the study populations at each time-point of the labelling period was compared across T cell subsets in all subjects ($n = 10$ T1D; $n = 10$ controls).

To calculate the replacement rate, k, we assumed that our cell subpopulations were kinetically homogeneous and disappearance of cell subsets from the blood follows a single-exponential decay equation [24,35], where $k = \frac{-\ln(1-f)}{t}$. An average of f measured on days 28–42 was used for this calculation.

Proliferation (p) and disappearance rates (d*)

Obtaining additional samples after the labelling period and measuring the plasma or total body water (TBW), ^2H enrichment allowed us to use mathematical models which do not require assumptions about disappearance kinetics in 10 subjects ($n = 4$ controls; $n = 6$ T1D) [32,36–38]. We estimated the average proliferation rate, p, of the subpopulation (including actively proliferating and quiescent subpopulations) and d*, the disappearance rate of labelled cells (the recently proliferated population). Proliferation rates, expressed as doubling time (t_2), and disappearance expressed as half-life ($t_{1/2}$), were calculated as ln2/p and ln2/d*, respectively. Model assumptions and parameter estimates are provided Appendix Tables A1–A3.

Table 1. Summary of study participants.

Subject	Gender	Age (years)	WBC (K/cmm)	Years with T1D	HbA1c (%)	Daily dose of ^2H_2O (ml)	Labelling period (days)	Samples collected after labelling period?
C1	F	19	5·5	–	–	60	42	No
C2	M	18	8·3	–	–	60	42	No
C3	M	19	5·3	–	–	60	42	No
C4	F	27	4·7	–	–	60	42	No
C5	M	38	4·4	–	–	60	42	No
C6	M	50	6·0	–	–	60	42	No
C7	F	56	7·8	–	–	80	63	Yes
C8	F	24	9·0	–	–	80	63	Yes
C9	M	28	5·5	–	–	80	63	Yes
C10	F	24	7·7	–	–	80	63	Yes
Mean ± s.d.		30 ± 13	6·4 ± 1·6					
DM1	M	24	4·7	21	7·8	60	42	No
DM2	M	32	6·5	15	7·2	60	42	No
DM3	M	33	4·4	27	7·1	60	42	No
DM4	M	30	10·5	3	7·8	60	42	No
DM5	F	24	6·7	15	8·3	80	42	Yes
DM6	F	35	4·7	24	7·7	80	42	Yes
DM7	F	27	6·0	14	–	80	63	Yes
DM8	M	40	8·1	8	7·8	80	48	Yes
DM9	M	34	7·5	18	–	80	44	Yes
DM10	M	49	7·8	43	8·3	80	63	Yes
Mean ± s.d.		33 ± 8	6·7 ± 1·9	19 ± 11	7·8 ± 0·4			

There were no significant differences between type 1 diabetes and control groups with respect to age ($P = 0·59$) and white blood cell (WBC) count ($P = 0·74$). Concurrent medications: C1: oral contraceptive; DM1-10: insulin; DM3: fish oil, aspirin; DM7: fluoxetine, oral contraceptive; DM8: insulin aspirin, paraxetine, bupropion, gabapentin, lisinopril, simvistatin; DM9: lisinopril, claritin, flonase; DM10: zonasamide; F: female; M: male; s.d.: standard deviation.

Statistical analyses

Unless noted otherwise, simple means were compared using the Mann–Whitney *U*-test and group means over time were compared using two-way analysis of variance (ANOVA). Differences were considered significant at $P \leq 0·05$. These statistical calculations were performed using GraphPad Prism 5 statistical software.

To quantify the variability in T cell fractions over time, we used a linear mixed model including a fixed-group effect (type 1 diabetes *versus* control) and random effect for each subject to estimate the intraclass correlation coefficient (ICC). The ICC is the proportion of the total variance explained by variability between subjects, while the proportion of variance that is due to within-subject variation is 1-ICC.

Results

Study subject characteristics

As shown in Table 1, study subjects were aged between 18 and 56 years. There were no significant differences between the T1D and control subjects with respect to mean age (33 years *versus* 30 years, $P = 0·59$) or baseline white blood cell count (6·7 K/mm^3 *versus* 6·4 K/mm^3, $P = 0·74$). The mean HbA1c in type 1 diabetes subjects was elevated at 7·8% and the mean duration of diabetes was 18·9 years. Mean T cell subset fractions (T_{reg}: 7% T1D *versus* 10% control, memory: 46% T1D *versus* control 43%, naive: 50% T1D *versus* 50% control) were similar between groups.

Composition of CD4$^+$T cell subsets were stable over the study period

The models that we use assume that there is minimal fluctuation in the pool size of the memory, naive and T_{reg} subsets over the time-period of the labelling experiment. As shown in Fig. 1c, the within-subject variation in T cell fractions is small compared to the between-subject variation ($ICC_{memory} = 0·80$, $ICC_{naive} = 0·81$ and $ICC_{Treg} = 0·64$), especially for the memory and naive cell populations, indicating that these are reasonably stable cell populations in the periphery with which to calculate proliferation and disappearance rates.

Granulocyte enrichment

Measures of turnover (f, k, p and d*) have been normalized by each individual's granulocyte enrichment to account for differences in deuterium availability across subjects. All subjects, regardless of the amount of deuterated water

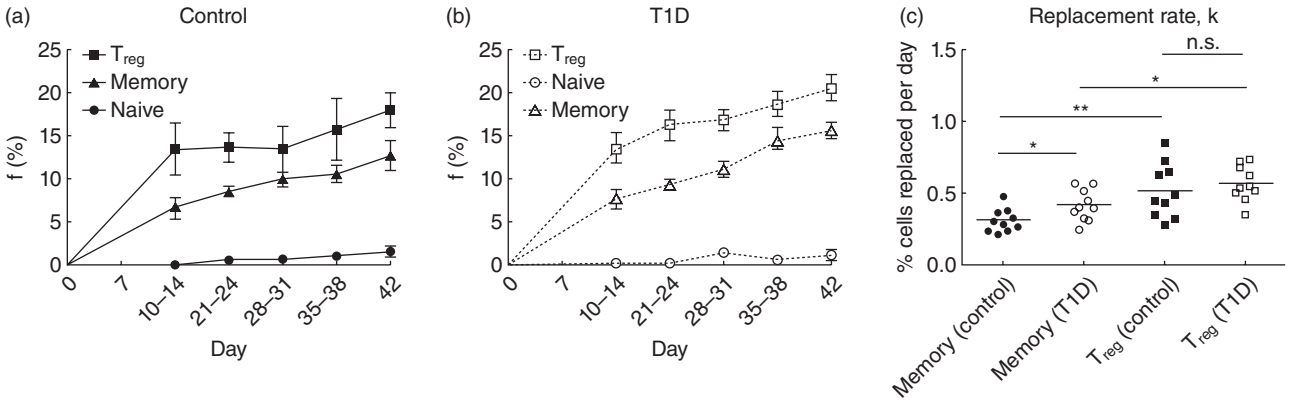

Fig. 2. Fractional enrichment (f) and calculated replacement rate (k) in all subjects. (a,b) Fractional enrichment, f, of regulatory T cells (T_{reg}) > memory>>naive in both control subjects (a: $n = 10$, $P < 0{\cdot}001$) and type 1 diabetes (T1D) subjects (b: $n = 10$, $P < 0{\cdot}001$). Group means over time compared using two-way analysis of variance (ANOVA). (c) Mean replacement rate, k. Control subjects ($n = 10$) T memory cells k = 0·31%/day, T1D subjects ($n = 10$) memory cells k = 0·42%/day (*$P < 0{\cdot}05$). Control subjects ($n = 10$) T_{reg} cells k = 0·52%/day and T1D subjects ($n = 10$) T_{reg} cells k = 0·57%/day (P = not significant (n.s.). Control subjects memory < T_{reg} ($P < 0{\cdot}01$); T1D subjects T memory < T_{reg} ($P < 0{\cdot}05$). Means compared using Mann–Whitney *U*-test. *$P < 0{\cdot}05$; **$P < 0{\cdot}01$.

prescribed by protocol, reached either plasma enrichment levels > 1·0% or granulocyte enrichment levels > 2·5% which have been shown previously to be sufficient for lymphocyte DNA incorporation analyses [33], and there were no differences between T1D ($n = 10$) and healthy control ($n = 10$) subjects (two-way ANOVA $P = 0{\cdot}98$; data not shown).

Comparisons of T cell subset within each disease group (controls and T1D)

As illustrated in Fig. 2a, among the healthy control subjects ($n = 10$) the fractional enrichment with deuterium (f) was greater in T_{reg} cells than $CD4^+$ memory cells and both were much greater than the naive cell population, indicating an increased rate of incorporation of deuterium into cellular DNA, thus a more rapid turnover of this T cell compartment. Similar findings were seen among those with T1D ($n = 10$) (Fig. 2b).

Comparisons of T cell kinetics between healthy controls and those with T1D

Our primary goal was to determine if T cell kinetics were different between healthy controls and those with T1D.

Replacement rate. Significant differences were seen between T1D ($n = 10$) and control ($n = 10$) subjects with respect to the calculated replacement rate (k) for $CD4^+$ memory cells, whereas no differences were found in (k) in the T_{reg} subset (Fig. 2c). In control subjects ($n = 10$) $CD4^+$ memory cell mean k = 0·31% per day, which corresponds to a doubling time (t_2) of 222 days. In the T1D subjects ($n = 10$) $CD4^+$ memory cell population k = 0·42% per day, or $t_2 = 164$ days, which is significantly faster than controls ($P = 0{\cdot}03$).

Proliferation and disappearance rates. Quantification of proliferation (p) and disappearance (d*) rates was possible only in subjects who had plasma and other samples obtained before and after the labelling period, as indicated in Table 1. Using the Asquith model described in the Appendix, these data demonstrate a higher (p) and (d*) in the $CD4^+$ memory T cells from T1D ($n = 6$) compared with control ($n = 4$) subjects and no difference in (p) and (d*) in the T_{reg} subset (Fig. 3a,b). The mean $CD4^+$ memory T cell proliferation rate was p = 0·36% per day, or equivalently $t_2 = 195$ days in controls *versus* 0·46% per day or $t_2 = 153$ days in T1D ($P = 0{\cdot}02$). The $CD4^+$ memory cell disappearance rate was also greater in T1D subjects (d* = 1·48% per day in controls, which corresponds to $t_{1/2} = 47$ days *versus* 1·92% in T1D, with $t_{1/2} = 37$ days, $P = 0{\cdot}002$), suggesting that $CD4^+$ memory cells were leaving the memory pool more rapidly in T1D subjects compared to controls.

Discussion

In vivo monitoring of the kinetics of immune cells is a potentially important tool for understanding the pathophysiology of autoimmunity and the immune response to various therapies. *In vivo* labelling of lymphocytes with stable isotopes in humans has been performed in the setting of ageing, infections and cancer but, to our knowledge, has not been performed in the setting of autoimmune disease. Here we have validated an *in vivo* protocol using deuterium oxide to measure the kinetics of T memory and T_{reg} cell populations in T1D and healthy control subjects. We found that turnover of $CD4^+$ memory cells was significantly faster in T1D subjects compared to control subjects using two different mathematical approaches. Our studies confirmed other reports, that turnover of T_{reg} is greater than memory cells in healthy control subjects [23,39,40], and demonstrate

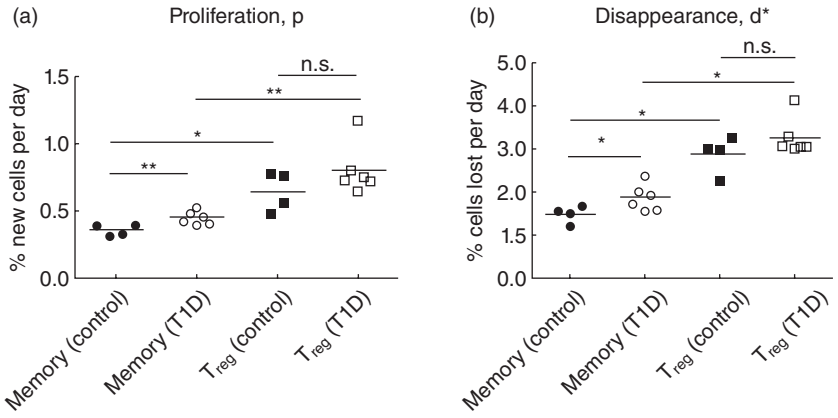

Fig. 3. Measures of T cell turnover in control and type 1 diabetes (T1D) subjects who had post-labelling samples collected. (a) Average proliferation rate, p. Control subjects memory cells mean p = 0·36%/day, T1D memory cells p = 0·46%/day (**$P < 0·01$); control subjects regulatory T cells (T_{reg}) cells mean p = 0·65%/day and T1D T_{reg} cells mean p = 0·91%/day (P = n.s.). (b) Disappearance rate, d*. Control subjects T memory cells mean d* = 1·48%/day, T1D memory cells d* = 1·92%/day (*$P < 0·05$); control subjects T_{reg} cells mean d* = 2·89%/day and T1D T_{reg} cells d* = 3·56%/day (P = n.s.). Means compared using Mann–Whitney U-test. *$P < 0·05$; **$P < 0·01$.

that this is also true in individuals with T1D. Incorporation of deuterium into naive cells was extremely low, although within the detection limits of our methods, suggesting an extremely slow turnover rate.

The significance of increased proliferation and disappearance rates of $CD4^+$ memory in T1D subjects is unknown. It is important to note that increased disappearance of $CD4^+$ memory cells in T1D *versus* controls reflects the labelled cells leaving the sampling pool. This could be due to cell death, transition to other cell types or migration from peripheral blood into tissues. Using static measurements, we were unable to demonstrate differences in the frequency of proliferating ($Ki67^+$, $CD38^+$) or dying (annexin V^+) memory cells between T1D and controls (Appendix Fig. A3). Previous work by Peakman, Roep and others has shown alterations in the frequency of $CD4^+$ memory effector cell populations in peripheral blood of T1D. As $CD4^+$ memory cell development is dependent upon T cell receptor (TCR) signal strength, antigen dose and the cytokine milieu [41–43], altered TCR signalling, persistent antigen and aberrant response to cytokines may all contribute to increased memory T cell turnover in T1D.

While it is possible that metabolic factors including peripheral hyperinsulinaemia and hyperglycaemia affect T cell kinetics, such an effect would be unlikely to explain our findings, which were limited to the $CD4^+$ memory subset. There was also no correlation between baseline HbA1c and turnover measures of T cell subsets within the group of T1D subjects studied. However, additional studies with a larger number of T1D subjects with a wider range of glycaemic control and/or comparison studies with type 2 patients are needed to understand more clearly the impact of metabolic factors on immune cell kinetics. Our finding of increased T memory cell turnover in T1D subjects many years from diagnosis is consistent with the notion suggested previously by others, that there is an ongoing inflammatory state in individuals living with T1D [12,19,44].

In our study, although there was a trend towards a greater turnover of T_{reg} in T1D compared to control subjects, we were unable to demonstrate significant differences between groups due potentially to the heterogeneity of our sorted T_{reg}. Although additional staining of available T_{reg} samples with FoxP3 yielded a reasonable purity of 83% (Appendix Fig. A1), Miyara [45], Booth [46] and others reported that within the T_{reg} population, there are naive quiescent T_{reg} ($CD4^+CD25^{low}CD45RA^+$) and rapidly dividing, activated T_{reg} ($CD4^+CD25^{high}CD45RO^+$), which we might expect to have differing kinetic profiles. As both cell types were considered together in our study, this may have limited our ability to detect differences in T_{reg} subsets between diabetes and control subjects. Future studies addressing these specific populations as well as central memory and effector memory subtypes may be informative.

The estimated T_{reg} and memory proliferation rates in our control subjects are lower than those published by Vukmanovic-Stejic *et al.* [23] and Macallan *et al.* [38]. This is attributable both to differences between studies in how the cell populations were defined and the isotope labelling technique chosen. The previous studies included $CD25^+$ cells within the memory pool and 127^+ cells within the T_{reg} pool, thus incorporating blasting population and activated memory cells with more rapid turnover. The slower turnover of memory cells in our study was due probably to limiting our memory population to $CD25^-$ cells which excludes a 'blasting' population. Similarly, by limiting our T_{reg} pool to $CD25^+127^{low}$ cells, we excluded activated memory cells which are known to proliferate and die quickly. Choice of isotope for DNA labelling and length of labelling protocol have been shown to impact estimated proliferation and death rates, with higher values being obtained with labelled glucose over labelled water and with shorter labelling times [37]. Assuming a model of 'kinetic heterogeneity', as we have in our estimation of p and d* (i.e. $p \neq d^*$), a longer labelling period allows for a greater proportion of cells with a slow turnover to be labelled, thus disappearance rates of labelled cells are expected to be higher in labelling experiments of short duration such as those employed by Vukmanovic-Stejic and Macallan.

A major goal in conducting these studies was to validate the use of heavy isotope labelling in individuals with T1D. Although our sample size was small, we confirmed the stability of T cell pool fractions over time in both T1D and healthy controls. We also confirmed that sufficient enrichment can be achieved in T1D subjects receiving deuterated water to enable adequate labelling of cells of interest. We were able to demonstrate increased turnover in $CD4^+$ memory cells using the calculated replacement rate (k) derived from the fractional enrichment (f), and were able to confirm these analyses using the Asquith model of proliferation (p) and disappearance (d*) rates which do not require assumptions about disappearance kinetics. Moreover, this technique was safe and well-tolerated. Application of heavy isotope labelling to understand T cell kinetics during the period prior to clinical disease or after immunotherapy is likely to enhance our understanding of T1D and the mechanisms involved in response to novel therapuetics.

Disclosure

This work was funded by the JDRF. The authors have no conflicts to report related to this work.

References

1 Makhlouf L, Grey ST, Dong V *et al*. Depleting anti-CD4 monoclonal antibody cures new-onset diabetes, prevents recurrent autoimmune diabetes, and delays allograft rejection in nonobese diabetic mice. Transplantation 2004; **77**:990–7.
2 Willcox A, Richardson SJ, Bone AJ, Foulis AK, Morgan NG. Analysis of islet inflammation in human type 1 diabetes. Clin Exp Immunol 2009; **155**:173–81.
3 Segurado OG, Arnaiz-Villena A, Wank R, Schendel DJ. The multifactorial nature of MHC-linked susceptibility to insulin-dependent diabetes. Autoimmunity 1993; **15**:85–9.
4 Mikulkova Z, Praksova P, Stourac P *et al*. Numerical defects in CD8+. Cell Immunol 2010; **262**:75–9.
5 Petersen LD, Duinkerken G, Bruining GJ, van Lier RA, de Vries RR, Roep BO. Increased numbers of *in vivo* activated T cells in patients with recent onset insulin-dependent diabetes mellitus. J Autoimmun 1996; **9**:731–7.
6 Hedman M, Faresjo M, Axelsson S, Ludvigsson J, Casas R. Impaired CD4 and CD8 T cell phenotype and reduced chemokine secretion in recent-onset type 1 diabetic children. Clin Exp Immunol 2008; **153**:360–8.
7 Peakman M, Mahalingam M, Leslie RD, Vergani D. Co-expression of CD45RA (naive) and CD45R0 (memory) T-cell markers. Lancet 1994; **343**:424.
8 Wildin RS, Freitas A. IPEX and FOXP3: clinical and research perspectives. J Autoimmun 2005; **25** (Suppl.):56–62.
9 Brusko T, Wasserfall C, McGrail K *et al*. No alterations in the frequency of FOXP3+ regulatory T-cells in type 1 diabetes. Diabetes 2007; **56**:604–12.
10 Tree TI, Roep BO, Peakman M. A mini meta-analysis of studies on CD4+CD25+ T cells in human type 1 diabetes: report of the Immunology of Diabetes Society T Cell Workshop. Ann NY Acad Sci 2006; **1079**:9–18.
11 Kukreja A, Cost G, Marker J *et al*. Multiple immuno-regulatory defects in type-1 diabetes. J Clin Invest 2002; **109**:131–40.
12 Long SA, Cerosaletti K, Bollyky PL *et al*. Defects in IL-2R signaling contribute to diminished maintenance of FOXP3 expression in CD4(+)CD25(+) regulatory T-cells of type 1 diabetic subjects. Diabetes 2010; **59**:407–15.
13 Alcina A, Fedetz M, Ndagire D *et al*. IL2RA/CD25 gene polymorphisms: uneven association with multiple sclerosis (MS) and type 1 diabetes (T1D). PloS ONE 2009; **4**:e4137.
14 Dendrou CA, Wicker LS. The IL-2/CD25 pathway determines susceptibility to T1D in humans and NOD mice. J Clin Immunol 2008; **28**:685–96.
15 Hakonarson H, Qu HQ, Bradfield JP *et al*. A novel susceptibility locus for type 1 diabetes on Chr12q13 identified by a genome-wide association study. Diabetes 2008; **57**:1143–6.
16 Todd JA, Walker NM, Cooper JD *et al*. Robust associations of four new chromosome regions from genome-wide analyses of type 1 diabetes. Nat Genet 2007; **39**:857–64.
17 Chen Q, Kim YC, Laurence A, Punkosdy GA, Shevach EM. IL-2 controls the stability of Foxp3 expression in TGF-beta-induced Foxp3+ T cells *in vivo*. J Immunol 2011; **186**:6329–37.
18 Koenecke C, Czeloth N, Bubke A *et al*. Alloantigen-specific *de novo*-induced Foxp3+ Treg revert *in vivo* and do not protect from experimental GVHD. Eur J Immunol 2009; **39**:3091–6.
19 Buckner JH. Mechanisms of impaired regulation by CD4(+)CD25(+)FOXP3(+) regulatory T cells in human autoimmune diseases. Nat Rev Immunol 2010; **10**:849–59.
20 Setoguchi R, Hori S, Takahashi T, Sakaguchi S. Homeostatic maintenance of natural Foxp3(+) CD25(+) CD4(+) regulatory T cells by interleukin (IL)-2 and induction of autoimmune disease by IL-2 neutralization. J Exp Med 2005; **201**:723–35.
21 Schwartz RH. Natural regulatory T cells and self-tolerance. Nat Immunol 2005; **6**:327–30.
22 Delovitch TL, Singh B. The nonobese diabetic mouse as a model of autoimmune diabetes: immune dysregulation gets the NOD. Immunity 1997; **7**:727–38.
23 Vukmanovic-Stejic M, Zhang Y, Cook JE *et al*. Human CD4+ CD25hi Foxp3+ regulatory T cells are derived by rapid turnover of memory populations *in vivo*. J Clin Invest 2006; **116**:2423–33.
24 Hellerstein M, Hanley MB, Cesar D *et al*. Directly measured kinetics of circulating T lymphocytes in normal and HIV-1-infected humans. Nat Med 1999; **5**:83–9.
25 Hellerstein MK, Hoh RA, Hanley MB *et al*. Subpopulations of long-lived and short-lived T cells in advanced HIV-1 infection. J Clin Invest 2003; **112**:956–66.
26 Neese RA, Misell LM, Turner S *et al*. Measurement *in vivo* of proliferation rates of slow turnover cells by 2H2O labeling of the deoxyribose moiety of DNA. Proc Natl Acad Sci USA 2002; **99**:15345–50.
27 Mohri H, Perelson AS, Tung K *et al*. Increased turnover of T lymphocytes in HIV-1 infection and its reduction by antiretroviral therapy. J Exp Med 2001; **194**:1277–87.
28 Defoiche J, Debacq C, Asquith B *et al*. Reduction of B cell turnover in chronic lymphocytic leukaemia. Br J Haematol 2008; **143**:240–7.
29 Defoiche J, Zhang Y, Lagneaux L, Willems L, Macallan DC. *In vivo* ribosomal RNA turnover is down-regulated in leukaemic cells in chronic lymphocytic leukaemia. Br J Haematol 2010; **151**:192–5.

30 Akbar AN, Vukmanovic-Stejic M, Taams LS, Macallan DC. The dynamic co-evolution of memory and regulatory CD4+ T cells in the periphery. Nat Rev Immunol 2007; **7**:231–7.
31 Vukmanovic-Stejic M, Agius E, Booth N *et al*. The kinetics of CD4+Foxp3+ T cell accumulation during a human cutaneous antigen-specific memory response *in vivo*. J Clin Invest 2008; **118**:3639–50.
32 Asquith B, Debacq C, Macallan DC, Willems L, Bangham CR. Lymphocyte kinetics: the interpretation of labelling data. Trends Immunol 2002; **23**:596–601.
33 Busch R, Neese RA, Awada M, Hayes GM, Hellerstein MK. Measurement of cell proliferation by heavy water labeling. Nat Protoc 2007; **2**:3045–57.
34 Collins ML, Eng S, Hoh R, Hellerstein MK. Measurement of mitochondrial DNA synthesis *in vivo* using a stable isotope-mass spectrometric technique. J Appl Physiol 2003; **94**:2203–11.
35 Macallan DC, Fullerton CA, Neese RA, Haddock K, Park SS, Hellerstein MK. Measurement of cell proliferation by labeling of DNA with stable isotope-labeled glucose: studies *in vitro*, in animals, and in humans. Proc Natl Acad Sci USA 1998; **95**:708–13.
36 Vrisekoop N, den Braber I, de Boer AB *et al*. Sparse production but preferential incorporation of recently produced naive T cells in the human peripheral pool. Proc Natl Acad Sci USA 2008; **105**:6115–20.
37 Asquith B, Borghans JA, Ganusov VV, Macallan DC. Lymphocyte kinetics in health and disease. Trends Immunol 2009; **30**:182–9.
38 Macallan DC, Asquith B, Zhang Y *et al*. Measurement of proliferation and disappearance of rapid turnover cell populations in human studies using deuterium-labeled glucose. Nat Protoc 2009; **4**:1313–27.
39 Macallan DC, Wallace D, Zhang Y *et al*. Rapid turnover of effector-memory CD4(+) T cells in healthy humans. J Exp Med 2004; **200**:255–60.
40 Wallace DL, Zhang Y, Ghattas H *et al*. Direct measurement of T cell subset kinetics *in vivo* in elderly men and women. J Immunol 2004; **173**:1787–94.
41 Park SO, Han YW, Aleyas AG *et al*. Low-dose antigen-experienced CD4+ T cells display reduced clonal expansion but facilitate an effective memory pool in response to secondary exposure. Immunology 2008; **123**:426–37.
42 Sun JC, Williams MA, Bevan MJ. CD4+ T cells are required for the maintenance, not programming, of memory CD8+ T cells after acute infection. Nat Immunol 2004; **5**:927–33.
43 Swain SL, Bradley LM, Croft M *et al*. Helper T-cell subsets: phenotype, function and the role of lymphokines in regulating their development. Immunol Rev 1991; **123**:115–44.
44 Schneider A, Rieck M, Sanda S, Pihoker C, Greenbaum C, Buckner JH. The effector T cells of diabetic subjects are resistant to regulation via CD4+ FOXP3+ regulatory T cells. J Immunol 2008; **181**:7350–5.
45 Miyara M, Yoshioka Y, Kitoh A *et al*. Functional delineation and differentiation dynamics of human CD4+ T cells expressing the FoxP3 transcription factor. Immunity 2009; **30**:899–911.
46 Booth NJ, McQuaid AJ, Sobande T *et al*. Different proliferative potential and migratory characteristics of human CD4+ regulatory T cells that express either CD45RA or CD45RO. J Immunol 2010; **184**:4317–26.

Appendix

We modelled the measured up- and down-labelling of plasma ^2H_2O enrichment, P(t), as a marker of deuterium availability for incorporation, where:

$$P(t) = f\left(1 - e^{-\delta t}\right) + \beta^* e^{-\delta t} \text{ during the label intake } (t \le \tau), \text{ and}$$

$$P(t) = \left[f\left(1 - e^{-\delta \tau}\right) + \beta^* e^{-\delta \tau}\right] e^{-\delta (t-\tau)}$$

after cessation of label intake ($t > \tau$), where t represents time in days, δ represents the turnover rate of body water per day, π is the fraction of ^2H_2O in drinking water and τ represents length of labelling period in days. Baseline plasma ^2H_2O enrichment $P(0) = \beta$, that is attained after the boost of label by the end of day 0, determined the initial conditions.

To model the enrichment of the deoxyribose moiety of adenosine in the DNA of our subpopulations, we assume identical reaction kinetics of hydrogen and deuterium and of labelled and unlabelled adenosines. Because the adenosine deoxyribose (dR) moiety contains seven hydrogen atoms that may be replaced with deuterium, we expect an amplification factor, $c > 1$, in the enrichment of dR in DNA relative to the plasma enrichment. To estimate c more accurately we measured enrichment of dR in a cell population that is known to have a rapid turnover with no evidence of kinetically distinct subpopulations, i.e. granulocytes, such that p, the average production rate of the cell population is assumed to equal d, the disappearance rate of labelled cells. Amplification factor has been characterized previously [26] $1 < c < 7$ and is typically between 2·5–4·0 when plasma enrichment levels are 1·0–1·5%.

Label enrichment of adenosine in the DNA of a population of cells was modelled by:

$$\frac{dl}{dt} = cpP(t)A - dl,$$

where l is the total amount of labelled adenosine in DNA and A is the total amount of adenosine in the DNA of that population. Normalizing the equation by the total amount of adenosine in the DNA, $L = l/A$ yields:

$$L(t) = cpf\frac{\left[\frac{\delta}{d^*}\left(1 - e^{-d^* t}\right) - \left(1 - e^{-\delta t}\right) + \frac{\beta}{f}\left(e^{-d^* t} - e^{-\delta t}\right)\right]}{\delta - d^*}$$

during the label intake ($t \le \tau$), and

$$L(t) = cpf\frac{\frac{\delta}{d^*}\left(e^{-d^*(t-\tau)}\right) - e^{-\delta t} - e^{-\delta(t-\tau)}) - e^{-\delta t} + \frac{\beta}{f}\left(e^{-d^* t} - e^{-\delta t}\right)}{\delta - d^*}$$

after labelling stopped ($t > \tau$). In this model, the constancy of pool size has been assumed but no assumption of equality between p and d* has been made. Estimates for δ, π and β derived from plasma enrichment measures are shown in Appendix Table A1. Parameter estimates of d* and cp are shown with confidence intervals for granulocytes in Appendix Table A2 and memory and regulatory T cells (T_{reg}) in Appendix Table A3. The measured deuterium enrichment and fitted curves are graphed in Appendix Fig. A2.

Table A1. Plasma parameter estimates with confidence intervals in subjects who had post-labelling samples collected.

		δ		Π		β	
Subject	τ	Estimate	95% CI	Estimate	95% CI	Estimate	95% CI
C7	63	0·0675	0·0296–0·1050	0·0156	0·0136–0·0176	0·0081	0·0013–0·0150
C8	63	0·0547	0·0375–0·0712	0·0206	0·0186–0·0227	0·0055	0·0000–0·0112
C9	63	0·0769	0·0416–0·1010	0·0142	0·0134–0·0158	0·0117	0·0070–0·0154
C10	63	0·0768	0·0601–0·0937	0·0170	0·0164–0·0177	0·0110	0·0084–0·0137
DM5	42	0·1980	0·0000–0·5203	0·0142	0·0126–0·0159	0·0078	0·0029–0·0126
DM6	42	0·0971	0·0364–0·1580	0·0109	0·0099–0·0112	0·0071	0·0054–0·0087
DM7	63	0·1047	0·0017–0·2078	0·0125	0·0114–0·0137	0·0133	0·0071–0·0195
DM8	48	0·0682	0·0000–0·1610	0·0115	0·0091–0·0140	0·0098	0·0035–0·0162
DM9	44	0·0344	0·0077–0·0611	0·0116	0·0061–0·0170	0·0124	0·0064–0·0185
DM10	63	0·0866	0·0559–0·1170	0·0139	0·0131–0·0147	0·0063	0·0027–0·0100

Parameters estimated with 95% confidence intervals (CI) using fitted excess M_{+1} (EM1) data for plasma enrichment. δ: turnover rate of body water per day, π: fraction of ^2H_2O in drinking water, β: baseline body water enrichment attained after priming dose of label by the end of day 1.

Table A2. Granulocyte parameter estimates for subjects with post-labelling samples.

	cp		d* = p		
Subject	Estimate	95% CI	Estimate	95% CI	c
C7	0·3169	0·265–0·369	0·0910	0·074–0·108	3·4813
C8	0·3810	0·297–0·465	0·1080	0·080–0·136	2·9227
C9	0·2608	0·168–0·367	0·0746	0·044–0·112	3·4946
C10	0·2112	0·160–0·262	0·0689	0·049–0·089	3·0653
DM5	0·2659	0·209–0·032	0·0682	0·048–0·088	3·8971
DM6	0·3596	0·203–0·517	0·1020	0·047–0·157	3·5255
DM7	0·2838	0·196–0·371	0·0875	0·056–0·120	3·2438
DM8	0·3012	0·176–0·426	0·0741	0·034–0·114	4·0670
DM9	0·2399	0·119–0·361	0·0695	0·026–0·112	3·4538
DM10	0·2882	0·206–0·370	0·0930	0·062–0·124	3·1006

Parameters estimated with 95% confidence intervals (CI) using fitted excess M_{+1} (EM1) data for granulocyte enrichment. d*: disappearance rate of labelled cells, c: amplification factor or likelihood of deuterium incorporation, p: average turnover rate or rate at which each adenosine residue replicates. cp and d* are estimated in the granulocyte model allowing for calculation of c for each subject. d* is assumed to equal p for granulocyte population known to have a very rapid turnover rate.

Table A3. $CD4^+$ T memory and regulatory T cells (T_{reg}) parameter estimates for cp and d*.

	$CD4^+$ T memory					$CD4^+$ T_{reg}				
	cp			d*		cp			d*	
Subject	Estimate	95% CI	p	Estimate	95% CI	Estimate	95% CI	p	Estimate	95% CI
C7	0·0114	0·0079–0·0148	0·0033	0·0155	0·0077–0·0233	0·0268	0·0171–0·0364	0·0077	0·0326	0·0179–0·0473
C8	0·0093	0·0075–0·0111	0·0026	0·0120	0·0075–0·0166	0·0164	0·0111–0·0217	0·0047	0·0301	0·0180–0·0422
C9	0·0137	0·0093–0·0183	0·0039	0·0151	0·0070–0·0241	0·0274	0·0212–0·0339	0·0078	0·0299	0·0215–0·0397
C10	0·0123	0·0114–0·0131	0·0040	0·0168	0·0148–0·0187	0·0147	0·0128–0·0165	0·0048	0·0228	0·0187–0·0267
DM5	0·0189	0·0167–0·0210	0·0048	0·0194	0·0155–0·0234	0·0253	0·0197–0·0309	0·0065	0·0306	0·020–0·0412
DM6	0·0161	0·0117–0·0205	0·0046	0·0158	0·0063–0·0253	0·0412	0·0314–0·0510	0·0117	0·0412	0·0272–0·0574
DM7	0·0109	0·0115–0·0315	0·0034	0·0204	0·0098–0·0311	0·0189	0·0140–0·0275	0·0058	0·0305	0·0125–0·0486
DM8	0·0215	0·0071–0·0148	0·0053	0·0237	0·0094–0·0379	0·0297	0·0166–0·0429	0·0073	0·0328	0·0143–0·0513
DM9	0·0152	0·0072–0·0232	0·0044	0·0188	0·0019–0·0358	0·0495	0·0190–0·0800	0·0143	0·0484	0·0093–0·0874
DM10	0·0128	0·0099–0·0156	0·0041	0·0173	0·0112–0·0233	0·0232	0·0145–0·0318	0·0075	0·0300	0·0158–0·0442

Parameters estimated with 95% confidence intervals (CI) using fitted excess M_{+1} (EM1) data for $CD4^+$ memory and T_{reg} enrichment. d*: disappearance rate of labelled cells, c: the amplification factor or likelihood of deuterium incorporation, p: average rate at which each adenosine residue replicates, are estimated together as 'cp' in our model. cp is divided by c from Appendix Table A2 to obtain p, which is plotted in Fig. 3 of the main text.

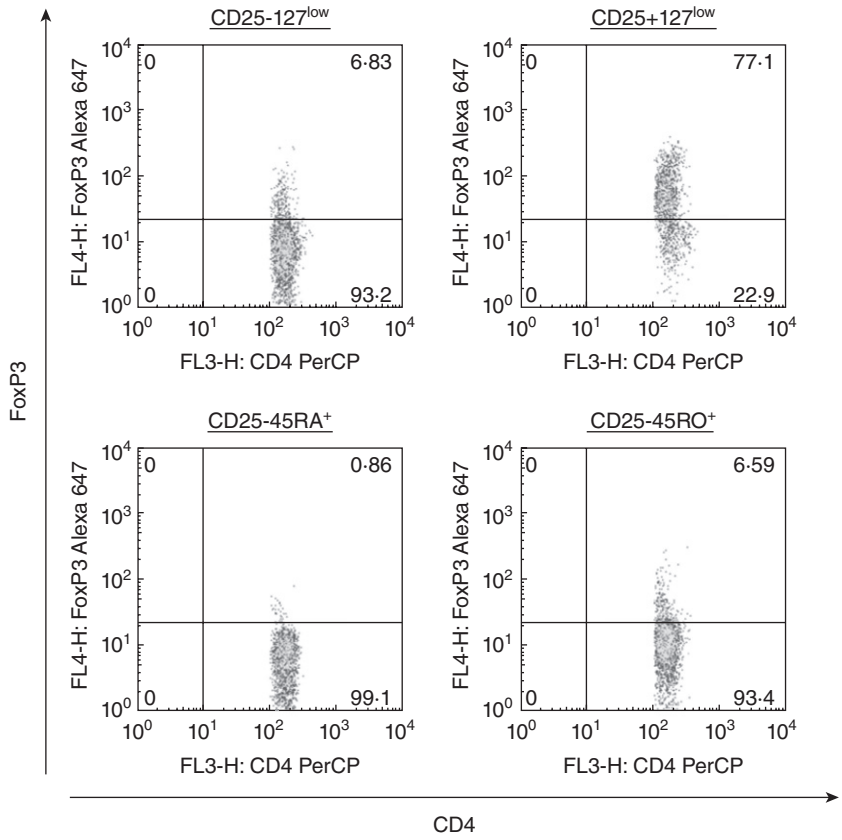

Fig. A1. Representative fluorescence activated cell sorter (FACS) plot with forkhead box protein 3 (FoxP3) staining.

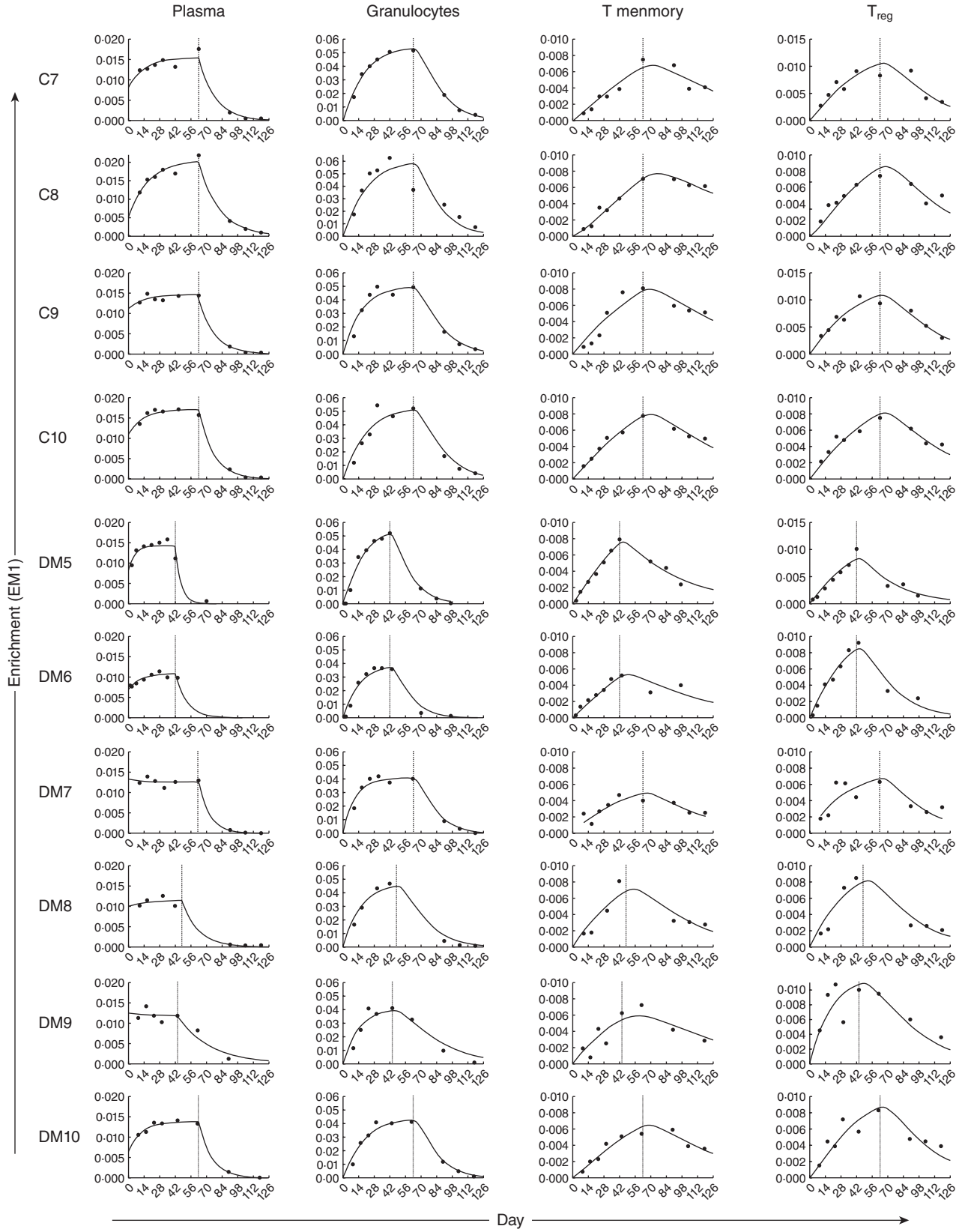

Fig. A2. Measured deuterium enrichment [excess M_{+1} (EM1)] with fitted curves for subjects from whom post-labelling samples were collected. To correct for the fraction of heavy water available in the body water, we fitted the measured label enrichment of plasma during up- and down-labelling, as described in the Methods. Measured enrichment (EM1) of plasma, granulocytes, T memory and regulatory T cells (T_{reg}) is plotted along with fitted curves for each subject. Vertical line represents last day of oral ^2H_2O consumption.

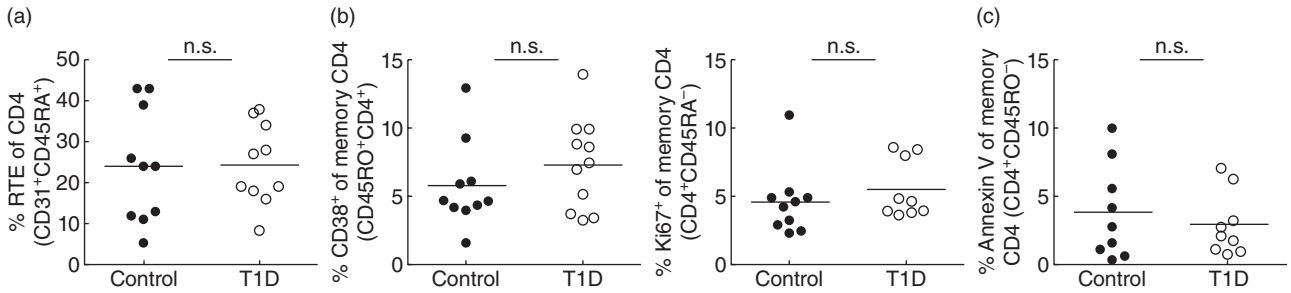

Fig. A3. Static measures of CD4 T cell composition and death. Age- and gender-matched peripheral blood mononuclear cells (PBMC) from control ($n = 10$) and type 1 diabetes (T1D) ($n = 10$) subjects were thawed, stained and analysed by flow cytometry for expression of markers of maturation, activation and death including (a) CD31 and CD45RA for recent thymic emigrants, (b) CD38 and Ki67 for proliferation and (c) annexin V for apoptosis. Black circles: control subjects; white circles: T1D subjects. Statistical differences were determined using a Student's *t*-test.